Computers and Geotechnics 124 (2020) 103605

Contents lists available at ScienceDirect

Computers and Geotechnics

journal homepage: www.elsevier.com/locate/compgeo

Research Paper

Computational modelling to predict the longevity of a permeable reactive barrier in an acidic floodplain

Subhani Medawela, Buddhima Indraratna*

Centre for Geomechanics and Railway Engineering, University of Wollongong, Wollongong, NSW 2500, Australia

ARTICLE INFO

Keywords:
Permeable reactive barriers
Bio-geochemical clogging
Acidic groundwater
Mineral precipitation
Transport modelling

ABSTRACT

This study introduces a novel computational approach that couples conventional geohydraulics with time-dependent changes of geochemical and biological parameters applied to a permeable reactive barrier (PRB) installed to treat acidified groundwater. The key objective of this PRB is to reduce excess acidity (low pH values), as well as to remove Al^{3+} and total Fe (i.e. Fe^{2+}, Fe^{3+}) from the acidic groundwater that flows through the PRB prior to being discharged as treated (neutralised) effluent to the environment. The governing equations characterising the geochemical reactions between the acidic influent and the alkaline PRB medium are incorporated into two finite-difference numerical codes, namely, MODFLOW and RT3D. In addition, biological clogging leading to reduced porosity of the PRB material over time is represented by explicit mathematical equations that are integrated with these geochemical numerical codes. The predictions from this coupled model made along the centreline of the PRB (i.e. one-dimensional flow) agree with the field data while demonstrating that the optimal treatment occurs predominantly in the proximity of the PRB inlet. The model also confirmed the potential benefit of using calcitic limestone (97% $CaCO_3$) in the PRB, where a lifespan of about 16 years can be expected.

1. Introduction

Groundwater flowing through acid sulfate soil terrains transports acidity (low pH) and toxic heavy metals (e.g. Al and Fe) that degrade the quality of the soil and associated water bodies [1]. Permeable reactive barriers (PRBs) consisting of alkaline aggregates (e.g. limestone, concrete) can release the alkalinity, neutralise the acidity, and remove the toxic metals from the groundwater by precipitation [2–5]. For example, in an alkaline environment, Fe and Al minerals precipitate as oxides and hydroxides. These solids accumulate in the voids of the granular medium of the PRB and reduce its porosity and permeability; referred to as chemical clogging of porous media [6–9]. Moreover, Al and Fe oxides and hydroxides form a coating that covers the entire surface of the reactive media, referred to as armouring [10].

Some groups of iron oxidising bacteria (IOB) living in pyritic terrains can accelerate the pyrite oxidation in acidic floodplains by five-to-six orders of magnitude more than the chemical oxidation of pyrite (FeS_2) [11,12] which causes the groundwater to acidify faster. IOBs enter the PRB with the groundwater and start to grow in the voids of the reactive porous media where the dissolved contaminants provide the required nutrients for biological growth. For instance, Fe^{2+} acts as the substrate for the particular IOB strain *Acidithiobacillus ferrooxidans,* which can grow inside the PRB when the pH of the environment is around 2 [13]. These biotic cells accumulate in the pores and block the flow path, hindering the full potential of the PRB. Meanwhile, *At. ferrooxidans* rapidly oxidises Fe^{2+} into Fe^{3+}, which increases the amount of iron oxides and hydroxides formed. Thus, biologically catalysed mineral precipitation and the accumulation of biomass in porous media result in fouling of the PRBs.

There has not been a comprehensive computational model to explain the phenomenon of time-dependent clogging by biological and geochemical mechanisms which adversely affect the longevity of a PRB in acidic ground. This study is focused predominantly on achieving this objective through a rigorous numerical analysis supported by field data over several years. This paper presents a bio-geochemical reactive transport model for field application developed using MODFLOW and RT3D software codes. After coupling the chemical and biological clogging mechanisms, a novel design criterion for PRBs is proposed, which is most beneficial when estimating the life span of a PRB. These predictions are essential during the design stage, especially for large-scale industrial applications with economic and environmental concerns. In this study, the performance of two PRBs was modelled; (i) PRB-1: a PRB filled with recycled concrete aggregates and located in the Shoalhaven acidic floodplain, NSW, Australia (Fig. 1) (ii) PRB-2: a newly proposed PRB which will be installed in the Shoalhaven acidic floodplain using limestone aggregates as the reactive material.

* Corresponding author.
E-mail addresses: skmsj997@uowmail.edu.au (S. Medawela), indra@uow.edu.au (B. Indraratna).

https://doi.org/10.1016/j.compgeo.2020.103605
Received 20 February 2020; Received in revised form 9 April 2020; Accepted 16 April 2020
Available online 06 May 2020
0266-352X/

Nomenclature

$\varnothing_k$	volume fraction of mineral
μ_g	gross specific growth rate [T^{-1}]
μ_{net}	net specific growth rate [T^{-1}]
ρ_c	solid phase biomass density [ML^{-3}]
Δn_t	porosity reduction at time Δt
$\hat{\sigma}_k^2$	variance of the lognormal random field $\hat{k}$
C	aqueous-phase concentration of contaminant [ML^{-3}]
C_o, C_1, C_2	Integral Constants
Da	Damkholer number
D_{ij}	Hydrodynamic dispersion coefficient [L^2T^{-1}]
h	Hydraulic head [L]
IAP	Ion Activity product
K	Hydraulic conductivity at time t [LT^{-1}]
k	Kinetic rate coefficient [$molm^{-3}s^{-1}$]
k_c	carrying capacity coefficient of a particular bacteria strain [T^{-1}]
K_{eq}	Solubility Constant for the reaction
K_o	Initial hydraulic conductivity [LT^{-1}]
K_T	Total number of species
$K_{\left(Fe^{2+}_{(aq)}\right)}$	Half saturation constant for ferrous [ML^{-1}]
K_{O_2}	Half saturation constant for oxygen [ML^{-1}]
K_{H^+}	Half saturation constant for hydrogen [ML^{-1}]
M_k	Mineral molar volume [m^3mol^{-1}]
N_m	Number of minerals
n_0	Initial porosity
n_t	Overall porosity reduction at time t
r	Reaction rate of each component [$molm^{-3}s^{-1}$]
$r_{[Fe^{2+}_{(aq)}]microbial}$	Rate of microbial iron oxidation [$molm^{-3}s^{-1}$]
R_k	Overall reaction rate for mineral dissolution and precipitation [$molm^{-3}s^{-1}$]
S	Substrate Concentration [ML^{-3}]
S_s	Specific storage of the porous material [L^{-1}]
t	Time [T]
W	Volumetric flux per unit volume representing sources and/or sinks of water [T^{-1}]
v_i	Seepage velocity [LT^{-1}]
X_o	Initial bacteria concentration [ML^{-3}]
X_s	Solid phase bacterial cell concentration [ML^{-3}]
X_∞	Maximum bacteria concentration [ML^{-3}]
Y	Yield coefficient

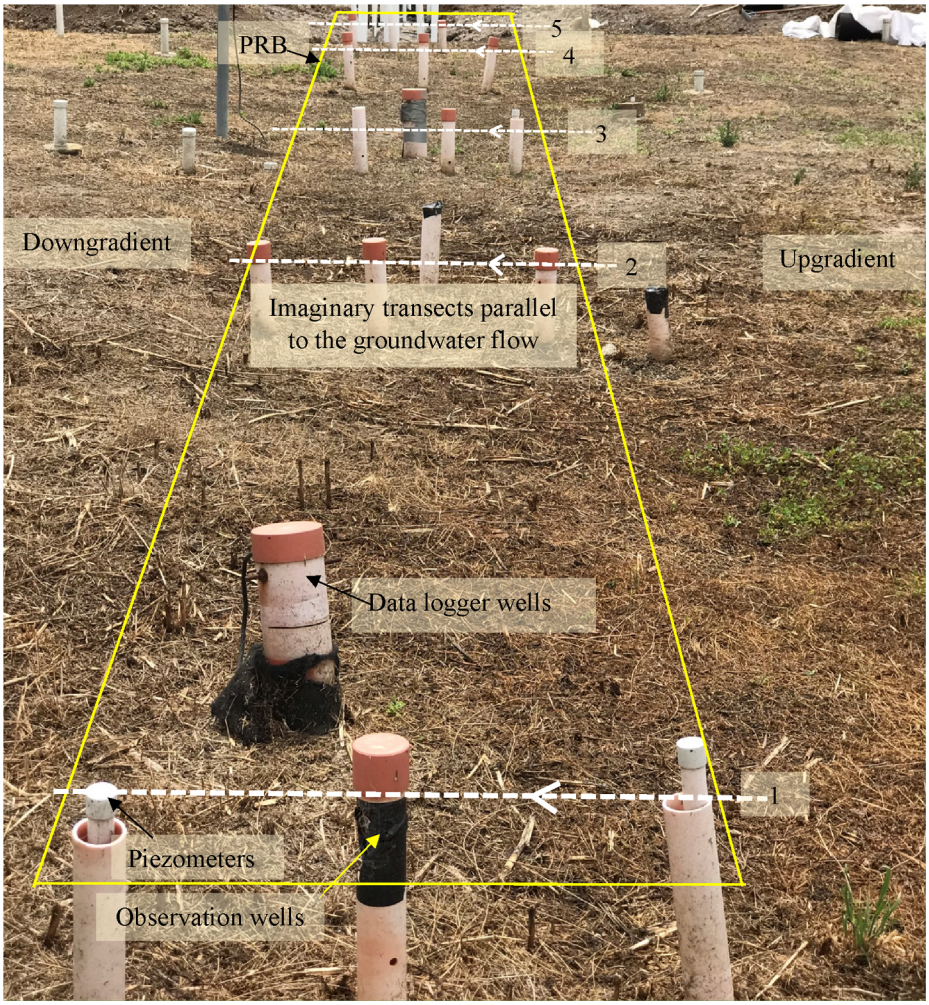

Fig. 1. Pilot-scale PRB (PRB-1) filled with recycled concrete in the Shoalhaven floodplain, Southeastern NSW, Australia (length = 18 m, width = 1.2 m, depth 3 m).

2. The bio-geochemical reactive transport model

A complete computational approach that combines the chemical and biological clogging in a PRB should be able to predict the temporal and spatial variations of the quality of groundwater when flowing along the PRB centreline, as well as the porosity and hydraulic conductivity of the reactive granular media within the PRB. The finite-difference model MODFLOW solves the following expression for three-dimensional movement of groundwater of a constant density through a porous earthen medium [14]:

$$\frac{\partial}{\partial x}\left(K_{xx}\frac{\partial h}{\partial x}\right)+\frac{\partial}{\partial y}\left(K_{yy}\frac{\partial h}{\partial x}\right)+\frac{\partial}{\partial z}\left(K_{zz}\frac{\partial h}{\partial z}\right)+W=S_s\frac{\partial h}{\partial t} \tag{1}$$

where K_{xx}, K_{yy}, and K_{zz} are the hydraulic conductivity values along the x, y, and z coordinate axes; h is the hydraulic head [L], W is the volumetric flux per unit volume representing sources ($W > 0$) and/or sinks ($W < 0$) of water [T^{-1}], S_s is the specific storage of the porous material [L^{-1}], and t is time [T].

RT3D is a finite-difference model that solves the general macroscopic equation describing the fate and transport of aqueous species in multi-dimensional saturated porous media as follows [15]:

$$\frac{\partial C}{\partial t}=\frac{\partial}{\partial x_i}\left(D_{ij}\frac{\partial C}{\partial x_j}\right)-\frac{\partial}{\partial x_i}(v_i C)+\frac{q}{\varnothing}C+R_K \tag{2}$$

where C is the aqueous-phase concentration of a chemical species [ML^{-3}], D_{ij} is the hydrodynamic dispersion coefficient [L^2T^{-1}], v_i is the seepage velocity [LT^{-1}], $\varnothing$ is the soil porosity, q is the volumetric flux of water per unit volume of aquifer representing sources and sinks [T^{-1}], and R_K is the rate of the reactions that occur in the aqueous phase [ML^3T^{-1}].

MODFLOW calculates the hydraulic head (h) and seepage velocity (v_i), which can then be input into RT3D to determine the concentrations of chemical species (C) of the water at a particular time step. Both MODFLOW and RT3D were operated in tandem to determine the temporal variation in pH and the dissolved concentrations of Al^{3+} and total Fe (Fe^{2+} and Fe^{3+}) in the PRB effluent and also identify the time at which effluent water quality degrades, representing longevity of the PRB.

RT3D has an option to introduce user-defined reaction modules that can be customised to simulate different types of reactive transport systems. In the current study, a new reaction module was compiled as a dynamic link library and then introduced into RT3D via FORTRAN subroutines. This new module incorporates all the chemical and biological reactions that occur in recycled concrete and limestone granular media when they continuously get exposed to acidic groundwater (Appendix A).

In a hybrid MODLFOW- RT3D model, after the porosity and hydraulic conductivity are provided for the first time step, the software cannot automatically update these values in every time step. Therefore, the following equations [16] were used to generate an array of time varied hydraulic conductivity and porosity and then subsequently introduced to the simulation as an input file.

$$n_t = n_0 - \Delta n_t \tag{3}$$

$$K = K_0\left[\frac{n_0-\Delta n_t}{n_0}\right]^3\Big/\left[\frac{1-n_0+\Delta n_t}{1-n_0}\right]^2 \tag{4}$$

$$\Delta n_t = \left[\left(\frac{X_s}{\rho_c}\right)+\sum_{k_T=1}^{N_m} M_k R_k t\right] \tag{5}$$

where n_t is the porosity at time t, n_0 is the initial porosity, Δn_t is the change in porosity at time t, K is the intrinsic hydraulic conductivity [LT^{-1}] at time t, K_0 is the initial hydraulic conductivity [LT^{-1}], X_s is the solid-phase concentration of bacterial cells [ML^{-3}], ρ_c is the solid-phase biomass density [ML^{-3}], M_k is the molar volume (m^3mol^{-1}) of a mineral, and R_k is the summation of individual reaction rates of mineral dissolution and precipitation as follows [7,16–18]:

$$r = -k\left(1-\frac{IAP}{K_{eq}}\right) \tag{6}$$

where IAP is the ion activity product, K_{eq} is the solubility constant, and k is the kinetic rate coefficient ($molm^{-3}S^{-1}$) for each reaction. The value of IAP/K_{eq} in Eq. (6) can be directly calculated using the software PHREEQC Interactive V.3.3.12 [19] by introducing the concentrations of Al^{3+}, total Fe, Ca^{2+}, Na^+, K^+, Mg^{2+}, Cl^-, $SO_4{}^{2-}$, pH, redox potential and the temperature of the solution as input parameters.

2.1. Determining kinetic rate coefficients of a PRB at the design stage (PRB-2)

The proposed bio-geochemical model can be used to predict the performance of the limestone medium in the field (PRB-2), and it requires field-scale kinetic rate coefficients. Indraratna et al. [16] determined the laboratory-scale kinetic rate coefficients (k) for a granular limestone assembly. Although the same chemical and biological reactions occur in the laboratory and a real-life PRB, the biochemical processes often accelerate during the laboratory simulations because the conditions are strictly controlled (e.g., constant pH, concentrations of Al^{3+}, total Fe and IOB in the influent, accelerated flowrates, usually smaller particle sizes, and constant temperature). Therefore, erroneous outputs may be obtained if the mineral dissolution and precipitation in a real-life PRB are modelled using the reaction kinetics measured in laboratory systems that differ from natural systems [20]. Therefore, scaling up the bio-geochemical rate kinetics calculated based on laboratory observations to the field-scale is essential before installing an expensive field application.

The volume averaging method has been used in previous studies to upscale the rate kinetics from small (laboratory) scale to large (field) scale [21,22]. The following equations were developed by Lichtner et al. [22] and Tartakovsky et al. [23] based on stochastic analysis, and in this current study, were used to scale up the kinetic rate coefficients for bio-geochemical reactions in advective-reactive transport in porous media. In a linear reaction where the stoichiometric coefficient $\alpha = 1$, the upscaled rate coefficient (k_{eff}) is given as follows [23]:

$$k_{eff} = 1-\frac{\hat{\sigma}_k^2 Da}{2} \tag{7}$$

where $Da = l/U$,is the Damkholer number, defined as the time it takes solute transported by advection with average velocity U to travel one correlation length l, and $\hat{\sigma}_k^2$ is the variance of the lognormal random field $\hat{k}$. In a non-linear reaction where the stoichiometric coefficient $\alpha = 2$, the upscaled kinetic rate coefficient is given by [23],

$$k_{eff\,(x,t)} = \frac{2}{\langle c\rangle - 1}\left[\langle c^2\rangle - 2\hat{\sigma}_k^2 Da\left(\langle c^3\rangle - \langle c\rangle\right) - 1\right] \tag{8}$$

The biological oxidation of ferrous (Fe^{2+}) into ferric (Fe^{3+}) iron is represented as follows:

$$Fe^{2+}_{(aq)} + \frac{1}{4}O_{2(aq)} + H^+_{(aq)} \xrightarrow{Bacteria} Fe^{3+}_{(aq)} + \frac{1}{2}H_2O \tag{9}$$

The rate of biological oxidation of Fe^{2+} into Fe^{3+} ($d[Fe^{2+}]/dt$) can

be calculated as follows:

$$\frac{d[Fe^{2+}]}{dt} = k_{bio}\left(\frac{[Fe^{2+}_{(aq)}]}{K_{(Fe^{2+}_{(aq)})} + [Fe^{2+}_{(aq)}]}\right)\left(\frac{[O_{2(aq)}]}{K_{O_2} + [O_{2(aq)}]}\right)\left(\frac{[H^+]}{K_{H^+} + [H^+]}\right) \tag{10}$$

where $[Fe^{2+}_{(aq)}]$, $[O_{2(aq)}]$ and $[H^+]$ are concentrations of ferrous ions, oxygen, and hydrogen, respectively, $K_{\left(Fe^{2+}_{(aq)}\right)}$, K_{O_2}, K_{H^+} are the half-saturation constants, and k_{bio} is the kinetic rate coefficient of the reaction.

The laboratory-determined k_{bio} can be scaled up using Eq. (7), and then the bio-catalysing effect on mineral precipitation in the field is captured by Eq. (10). According to Monod [24], the rate of substrate utilisation by bacteria, i.e., the rate of Fe^{2+} oxidation which acts as the substrate for *At. ferrooxidans* growth can be calculated as follows:

$$\frac{d[Fe^{2+}]}{dt} = \frac{dS}{dt} = \frac{1}{Y}\frac{dX_s}{dt} \tag{11}$$

where S is the concentration of substrate (Fe^{2+}), and Y is the yield coefficient which was 1.42×10^{10} cells/g substrate. By knowing the rate of substrate utilisation in the field-scale via Eq. (10), the growth rate of bacteria (dX_s/dt) in the field-scale also can be calculated based on Monod kinetics using Eq. (11).

According to the stoichiometric coefficients of mineral dissolution and precipitation in each reaction occurring inside a limestone column (Appendix A), up-scaled reaction rates for the proposed PRB-2 were evaluated using Eqs. (7)–(11). The lab-scale rate coefficients were always higher than the field-scale values by almost three orders of magnitude (Table 1), which is why scaling up is necessary when applying the proposed model for field application. The up-scaled kinetic rates were introduced into the user-defined module in hybrid MODFLOW- RT3D finite-difference model via a FORTRAN subroutine (Appendix B).

2.2. Determining reaction rate coefficients of an existing PRB (PRB-1)

PRB-1, located in the Sholhaven acidic floodplain, NSW, Australia, was installed in 2006. It has been monitored continuously over the past 13 years by an on-site monitoring network of observation wells, data loggers, and piezometers (Fig. 1). The novel bio-geochemical reaction transport model can be used to evaluate the longevity and the correct time for maintenance of an existing PRB. If accurate laboratory-scale reaction kinetics are available, Eqs. (7)–(11) can be used to upscale those small-scale kinetic rate coefficients. Indraratna et al. [7] determined laboratory-scale kinetic rate coefficients (k) for a recycled concrete medium, ignoring the biotic role in PRB-1. They assumed that chemical clogging was the sole contributor to the PRB becoming clogged. Nevertheless, the presence of IOBs in the Shoalhaven terrain has been confirmed in the previous studies [16]. Therefore, scaling up the same laboratory kinetics determined by Indraratna et al.[7], and using them in the current numerical model to predict the actual PRB behaviour may be erroneous. In that case, field observations of an existing PRB can also be used to determine the field-scale kinetic rate coefficients as elaborated subsequently.

Firstly, the algorithm used by Indraratna et al. [16] to capture all the bio-geochemical reactions occurring in a granular limestone assembly was modified in this study to incorporate biologically catalysed chemical reactions occurring in a recycled concrete medium (see Appendix A). Then, kinetic rate coefficients (k) of individual reactions occur inside a recycled concrete granular assembly in field-scale were estimated. Next, exact kinetic rate coefficients were determined by calibrating the mathematical model developed by Indraratna et al. [16] as follows:

$$h(x,\ t) = (C_1 sinC_o x + C_2 cosC_o x).e^{F(t)} \tag{12a}$$

where

$$F(t) = \frac{-C_o^2}{B}\left(-\frac{\sum_{k=1}^{N_m} M_k R_k t^2}{2} + \frac{X_\infty}{\rho_c K_c} ln\left[1 - \frac{X_0}{X_\infty}(1 - e^{k_c t})\right] + (n_o + 2)t - 3ln[f(t) - n_o + 1] + 3ln\left[\frac{X_0}{\rho_c} - n_o + 1\right] + \frac{1}{f(t) - n_o + 1} - \frac{1}{\left(\frac{X_0}{\rho_c} - n_o + 1\right)}\right) \tag{12b}$$

$$f(t) = \sum_{k=1}^{N_m} M_k R_k t + \frac{X_0 X_\infty e^{k_c t}}{\rho_c\{X_\infty - X_0(1 - e^{k_c t})\}} \tag{12c}$$

Eq. (12) determines the hydraulic head at time t at a point located a distance x from the inlet of the PRB. Calibration was done so that the hydraulic head obtained by Eq. (12) corroborated with the head measured within PRB-1 using piezometers (Table 1).

The need to determine several kinetic rate coefficients ($k_{CaCO_3}, k_{AlOH_3}, k_{FeOH_3}, k_{FeOOH}, k_{Fe_2O_3}, k_{che}, k_{bio}$) for each and every grid cell of the model domain by trial-and-error approach for a number of years is time-consuming. Previous laboratory observations and geochemical analysis have proved that the optimum treatment of the PRB (hence the maximum reaction rate) occurs mainly at the inlet [7,16]. Therefore, following a conservative approach to determining the longevity of a relatively small pilot-scale PRB, the authors have determined the maximum values of kinetic rate coefficients for the inlet and considered them to be unchanged along the PRB centreline (one-dimensional flow path of the model). This approach enables an acceptable prediction of the earliest possible time for the effluent water quality to degrade.

3. Application of the model into an existing PRB (PRB-1)

3.1. Model domain

PRB-1 is filled with nearly uniform-sized recycled concrete aggregates, i.e. d_{50} = 40 mm [7,25], and the uniformity coefficient is 1.8. Therefore, within the granular mass, the unit weight and void ratio upon compaction (e = 0.5) are not expected to vary much irrespective of the direction. In this regard, modelling the aquifer as being homogeneous and isotropic is justifiable for simplicity. In the past, Indraratna

Table 1
Kinetic rate coefficients (k)in laboratory scale and field-scale.

Kinetic rate coefficients ((k) mol/Ls	Limestone		Recycled concrete	
	Laboratory [16]	Field	Laboratory [7]	Field (see Appendix A)
$CaCO_3(k_{CaCO_3})$	2.43E−07	7.21E−08	2.27E−07	3.81E−08
$AlOH_3(k_{AlOH_3})$	3.03E−07	8.98E−08	6.86E−07	9.70E−08
$Fe(OH)_3(k_{FeOH_3})$	8.98E−08	2.81E−08	5.87E−08	2.68E−08
$FeOOH(k_{FeOOH})$	8.49E−08	2.56E−08	5.87E−08	2.17E−08
$Fe_2O_3(k_{Fe_2O_3})$	7.81E−08	2.62E−08	5.87E−08	3.01E−08
Fe^{2+} aerobic oxidation(k_{che})	5.62E−08	1.97E−08	–	1.72E−08
Microbial Iron Oxidation(k_{bio})	3.09E−07	9.82E−08	–	8.79E−08

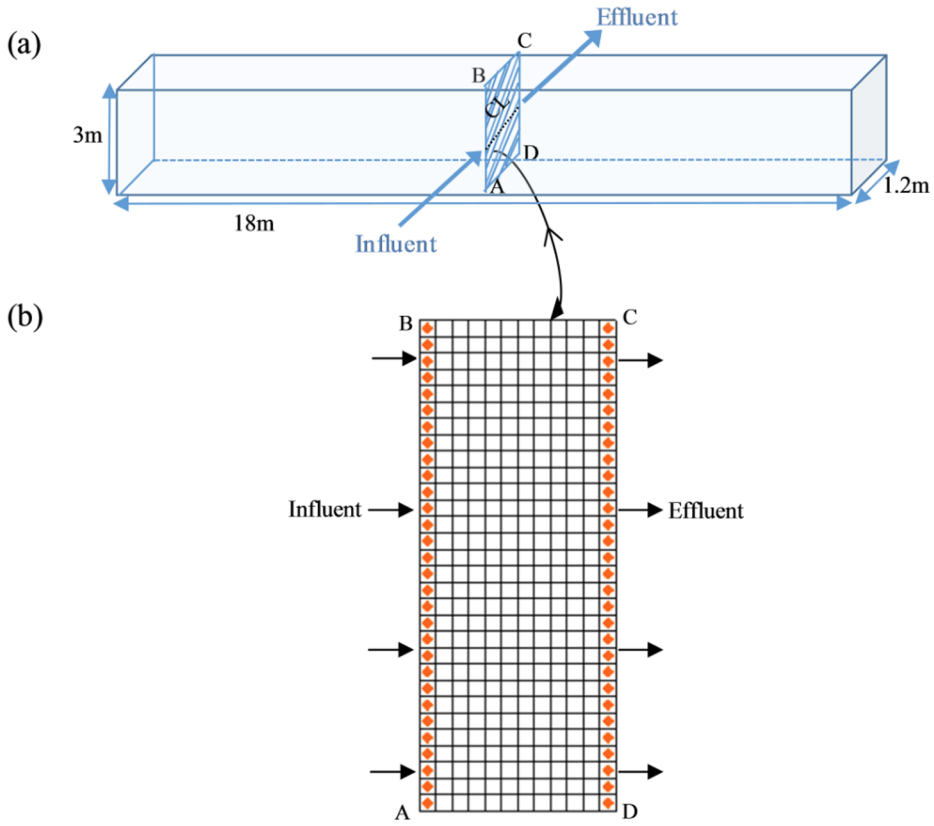

Fig. 2. (a) Layer through the centreline of the PRB (b) Model domain for ABCD Layer.

et al. [7] and Li and Benson [17] have also used the same assumptions for modelling chemical clogging of PRBs. As shown in Fig. 2a, a layer of unit thickness (ABCD) along the centreline of the PRB in the groundwater flow direction was considered in the model. The authors have assumed that there are no crossflows or flow divergence away from the centreline, i.e. crossflows or flow divergence away from the centerline were considered to be negligible. The PRB can be sliced into several vertical layers, similar to ABCD (1.2 m × 3 m), across the entire length of the PRB, which represents a model domain of 12 × 30 grid cells, as shown in Fig. 2b. When the vertical and lateral flows are assumed to be minimal, the one-dimensional horizontal flow through this layer can be assessed. By adding a number of identical ABCD layers next to each other, horizontal flow through the full length of the PRB can be represented. The inlet and outlet were considered to be specific head boundaries at the beginning (AB and CD sides), whereas both sides of the layer (the AD and BC sides) were considered to be no-flow boundaries. Wells with positive flow rates were defined at the inlet boundary to introduce flow into the domain.

3.2. Model input parameters

The lowest pH and the maximum concentrations of contaminants (dissolved Al^{3+} and total Fe) recorded during the preliminary site investigations at the Shoalhaven floodplain [25–27] were introduced as a constant model input (Table 2) throughout the simulation. Despite the constant model inputs, in reality, the up-gradient water quality (pH, Al^{3+} and total Fe) in the PRB influent fluctuated over time according to the environmental conditions [25]. However, by using the maximum possible concentration of contaminants as the model input, conservative predictions regarding the earliest time at which the effluent water quality begins to degrade were made.

3.3. Model predictions on acid neutralising by PRB-1

Fig. 3 compares the pH variations of water specimens taken along the centreline of PRB-1 (Transect 3 in Fig. 1) with the model predictions. The pH in PRB-1 was initially elevated to ~10 due to the initial

Table 2
Input parameters for bio-geochemical reactive transport model.

Input parameter	Unit	Value
Influent pH		3.4
Initial Porosity (n_0)		0.5
Flow rate	L/year	1.1×10^6
Initial hydraulic conductivity (K_0)	m/d	0.9565
Top elevation of the layer	mm	50
Bottom elevation of the layer	mm	0
Ca^{2+} of influent	mg/L	152
Fe^{3+} of influent	mg/L	49
Fe^{2+} of influent	mg/L	91
Al^{3+} of influent	mg/L	54
Bacteria Concentration of influent	cells/ cm^3	1×10^7
Initial Ca^{2+} of the aquifer(limestone)	mg/L	700
Initial Ca^{2+} of the aquifer(recycled concrete)	mg/L	550
Initial Fe^{3+} of the aquifer	mg/L	0
Initial Fe^{2+} of the aquifer	mg/L	0
Initial Al^{3+} of the aquifer	mg/L	0
Initial Bacteria Concentration of the aquifer	cells/ cm^3	0
Kinetic rate coefficients ((*k*)	mol/L.s	See Table 1

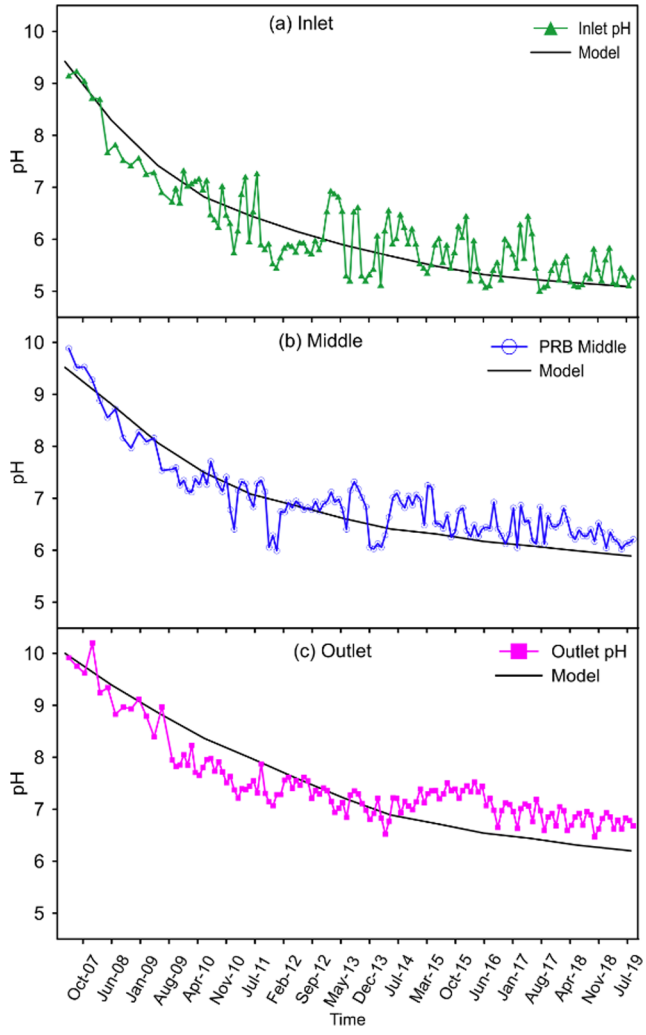

Fig. 3. Measured and model predicted pH from 2006 to 2019 along the centreline of PRB-1 (a) Inlet (b) Middle (c) Outlet.

dissolution of minor amounts of Ca bearing mineral in concrete and releasing hydroxyl and carbonate alkalinity while reaching equilibrium (Fig. 3). However, the pH gradually decreased because the carbonate alkalinity was not strong enough to maintain the peak pH for an extended period. Indraratna et al. [25] noted that these continuous reductions in pH were due to the armouring of aggregates, especially at the inlet of PRB-1, which hindered the release of Ca bearing minerals from the concrete and hence reduced the alkalinity within the system. The model accurately predicted the initial peak pH, although there were slight deviations afterwards. Starting from 2012, the pH at the inlet varied between 5 and 6.5, whereas the values predicted by the model were within that exact range until 2016 (Fig. 3a). Then, the pH predicted by the model gradually decreased while the observed values at the inlet fluctuated between 5 and 6. The continuous reduction in pH stems from the constant input acidity resulting in a faster degradation of water quality at the inlet during the final time steps (Fig. 3a). For instance, the average pH in 2019 at the inlet of PRB-1 was 4.16 versus the model input pH of 3.4. Therefore, the actual treatment at the PRB inlet was better than predicted for the final years of the monitoring period.

Bio-geochemical clogging and armouring in a porous granular assembly is not homogeneous along the flow path but rather reduces towards the outlet [16]. Therefore, the pH of the middle and outlet regions (Fig. 3b and c) was higher than that at the inlet (Fig. 3a). In these zones, pH predicted by the model was sufficiently accurate until 2014, but then the model results deviated slightly from the actual acidity. This deviation occurred because the actual input acidity to PRB-1 fluctuated despite the constant input to the model. Also, when non-homogeneous treatment occurred and partially treated water flowed into successive regions, the rates of Ca dissolution, the release of alkalinity and the formation of precipitates within PRB-1 changed, even though the kinetic rate coefficients determined for PRB-1 inlet were applied along the entire length of the model domain. Finally, porosity and hydraulic conductivity were introduced into the model at every time step by assuming a homogeneous and maximum reduction of these parameters along the centreline. However, in reality, the reductions in porosity and hydraulic conductivity were lower in the middle and outlet regions than at the inlet [16]. Therefore, the application of homogeneous model parameters throughout the domain caused the model to predict a lower pH than was measured in the middle and outlet regions, even though this resulted in predictions within adequate safety margins. The differences between the predicted and actual levels of pH increased towards the outlet region, and these deviations increased over time when the differences caused by the aforementioned factors accumulated. Since the deviation in pH predictions in the middle and outlet regions was only 4.8% and 6.2% in August 2019, after 13 years of operation, the model performed well overall.

3.4. Model predictions on metal removal

The model predicted the concentration of dissolved total Fe at the inlet accurately, despite slight fluctuations in the middle and end zones, especially during the final stage of data collection (Fig. 4a). Starting from 2015, i.e. after nine years of operation, the predicted concentrations of dissolved total Fe were higher than the measured values. For example, in August 2019, the deviations of model predictions at the inlet, middle, and end zones were 4.4%, 7.8% and 19.5%, respectively. After 2015, the predicted concentrations of dissolved Al^{3+} also began to increase more than the measured values, such that in August 2019 the deviations in the model predictions were 6.8%, 7.4% and 16.7% at the inlet, middle and end zone, respectively (Fig. 4b). The actual rate at which dissolved Al^{3+} and total Fe was removed should be less than the predicted rate due to the reasons explained previously (Section 3.3).

3.5. Longevity of PRB-1

Fig. 5 shows the predicted pH in the ABCD layer passing through the centreline of PRB-1. The pH at the outlet was predicted to decrease to 7.98 after five years (Fig. 5b), and 6.87 after 10 years (Fig. 5c). Since these pH values are almost neutral, the recycled concrete granular assembly is expected to remove excess acidy during these years. However, in the 11th year, the pH at the outlet is predicted to be acidic (Fig. 5d), and this acidity will increase further in the 13th year (Fig. 5e). The model results, therefore, suggested the PRB will generate an almost neutral effluent only for the first 10 years after the installation.

Fig. 6 shows that the predicted concentration of total Fe at the outlet to be less than 0.5 mg/L (ANZECC guidelines for Fe in surface water bodies [28]) until the 10th year, followed by an increase beyond the standards starting from the 11th year (Fig. 6d). These results predict that the PRB will generate iron-free effluent during the first 10 years. Similarly, the predicted concentration of Al^{3+} at the outlet is 0.51 mg/L

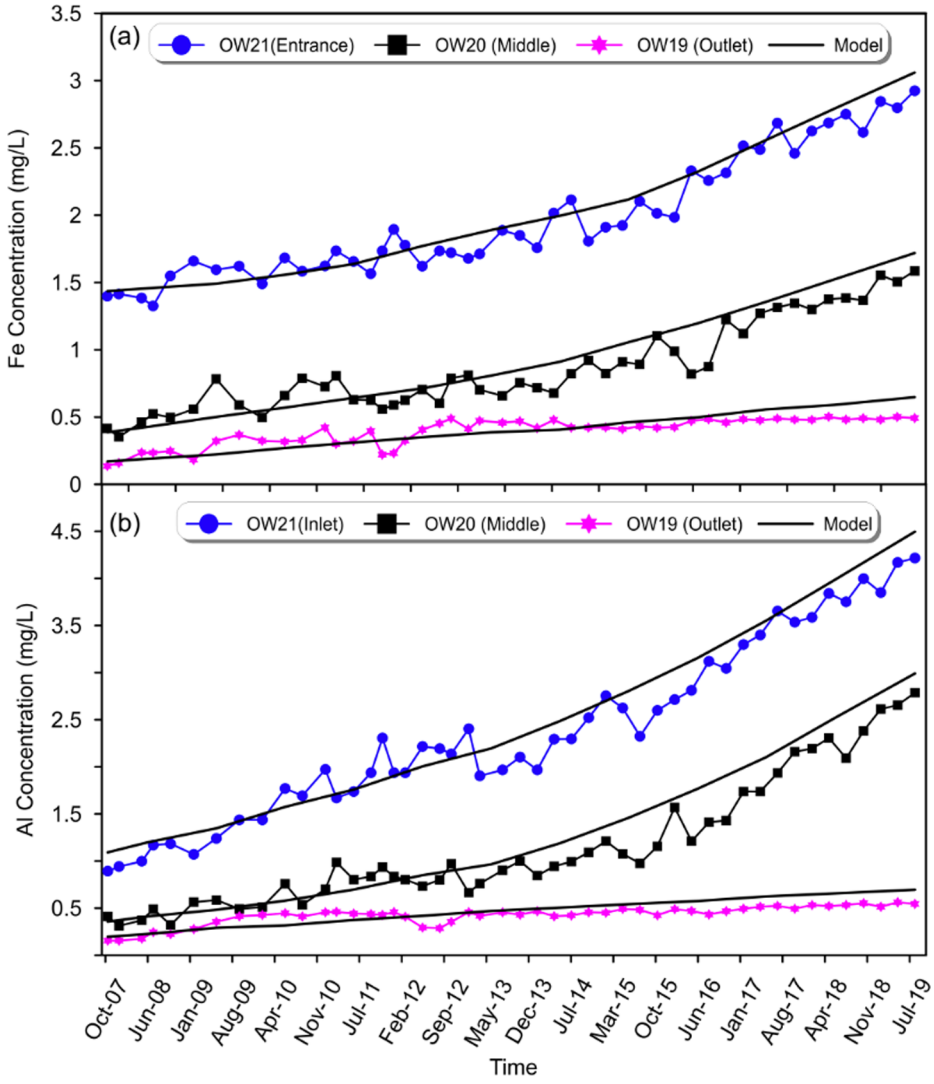

Fig. 4. (a) Measured and predicted dissolved metal concentration along the centreline of PRB-1 (a) total Fe (b) Al^{3+}.

after a decade (Fig. 7c), which is acceptable according to the ANZECC criteria ([Al] = 0.54 mg/L in water bodies [28]), but is expected to increase to 0.62 mg/L in the following year (Fig. 7d). Therefore, the PRB is expected to generate an effluent that is free of total Fe and Al^{3+} for the first 10 years.

In conclusion, the effective lifespan of PRB-1 is considered to be about 10 years, because the effluent is expected to be free of contaminants during this period. Subsequently, the effectiveness of treatment is expected to diminish as the reactive material in PRB-1 is chemically consumed over time. Nevertheless, field measurements showed that, although the pH had begun to decrease slowly, the effluent was still almost neutral (Fig. 3). The concentrations of Al^{3+} and total Fe were within the acceptable limits, even after 13 years (Fig. 4), verifying the conservative predictions made by applying the maximum concentrations of contaminants and reaction rates along the centreline of the PRB.

4. Predicting the longevity of a PRB at the design stage (PRB-2)

The initial dimensions of the proposed PRB-2 that will be installed in the Shoalhaven acidic floodplain are 18 m long × 1.2 m wide × 3 m deep. 1D flow along the centreline of PRB-2 was simulated to analyse the removal of acidity and metals from the groundwater flowing through a porous limestone media over 20 years. Model domain and input parameters were similar to those used for modelling PRB-1(Section 3).

Fig. 8 shows the variations in the concentrations of total Fe in the ABCD layer at different time steps. At the end of the 1st year, the predicted concentration of total Fe at the outlet (CD side) of the proposed PRB is 0.15 mg/L (Fig. 8a), and it increases to 0.44 mg/L (Fig. 8d) within 16 years. After 17 years, the predicted concentration of total Fe at the outlet is greater than 0.5 mg/L (Fig. 8e), which is the acceptable concentration for the amount of total Fe in surface water bodies based on ANZECC guidelines [28]. Therefore, the efficiency with which the granular limestone assembly can produce iron-free effluent decreases after 16 years. As Fig. 9 shows, in the 17th year of operation, the predicted concentration of Al^{3+} at the outlet increases to 0.57 mg/L, which exceeds the ANZECC guidelines (i.e. 0.54 mg/L). Therefore, the effluent from proposed PRB is predicted to be free of Al^{3+} and total Fe over the first 16 years.

According to the model predictions, the initial pH of the effluent rises to 8.67 (Fig. 10a), and then eventually reduces to 6.75 within

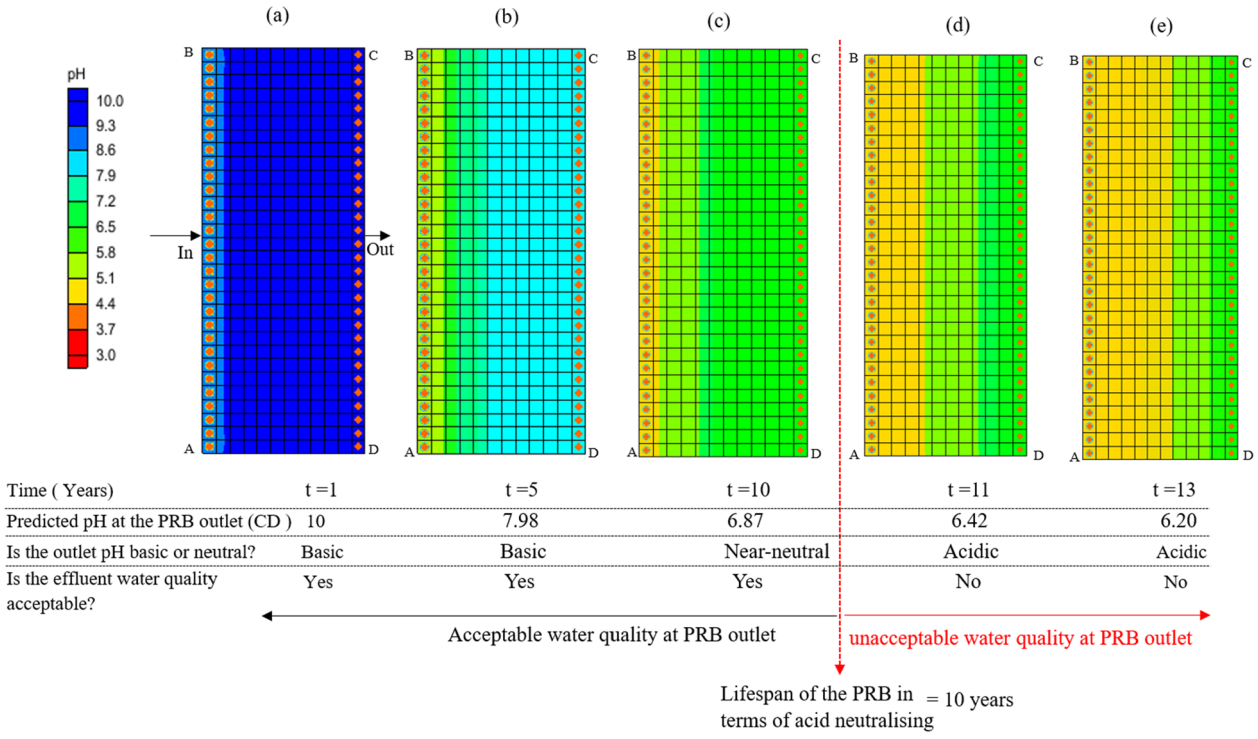

Fig. 5. Longevity prediction of PRB-1 (recycled concrete) based on the acid neutralising properties (a) variation of the pH in ABCD layer at the end of 1st year (b) 5th year (c) 10th year (d) 11th year (e) 13th year.

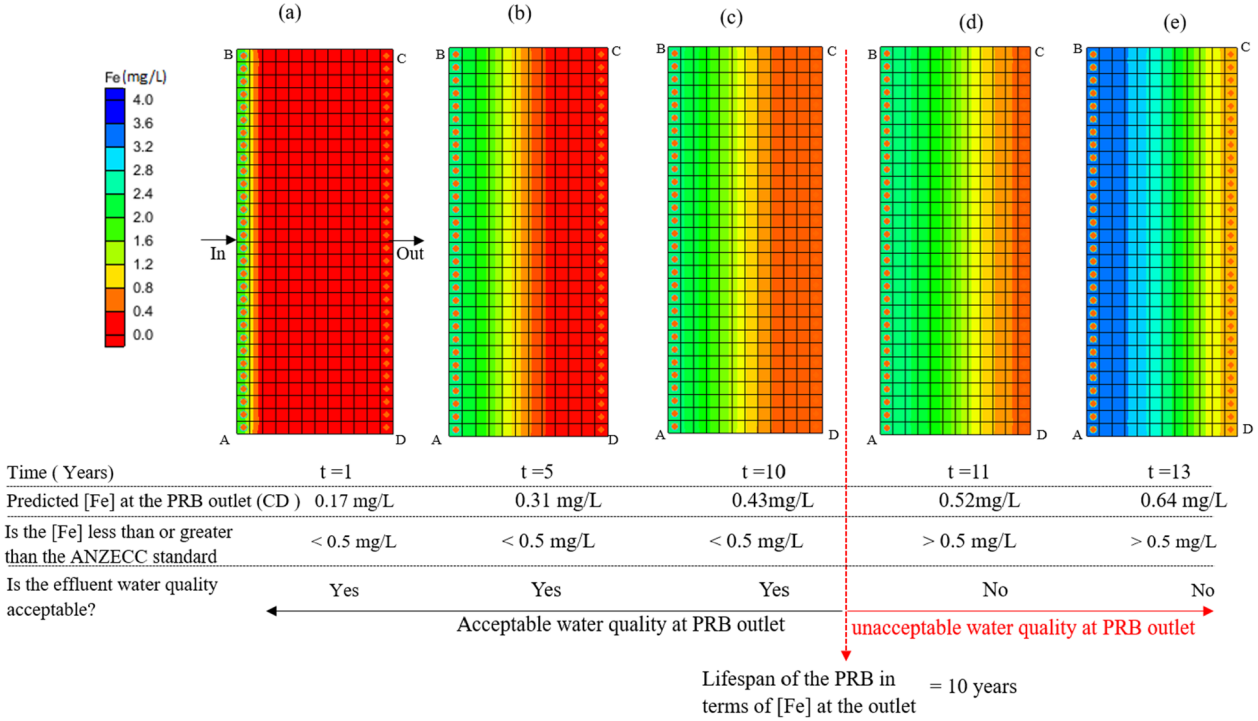

Fig. 6. Longevity prediction PRB-1 (recycled concrete) based on total Fe concentration (a) variation of [total Fe] in ABCD layer at the end of 1st year (b) 5th year (c) 10th year (d) 11th year (e) 13th year.

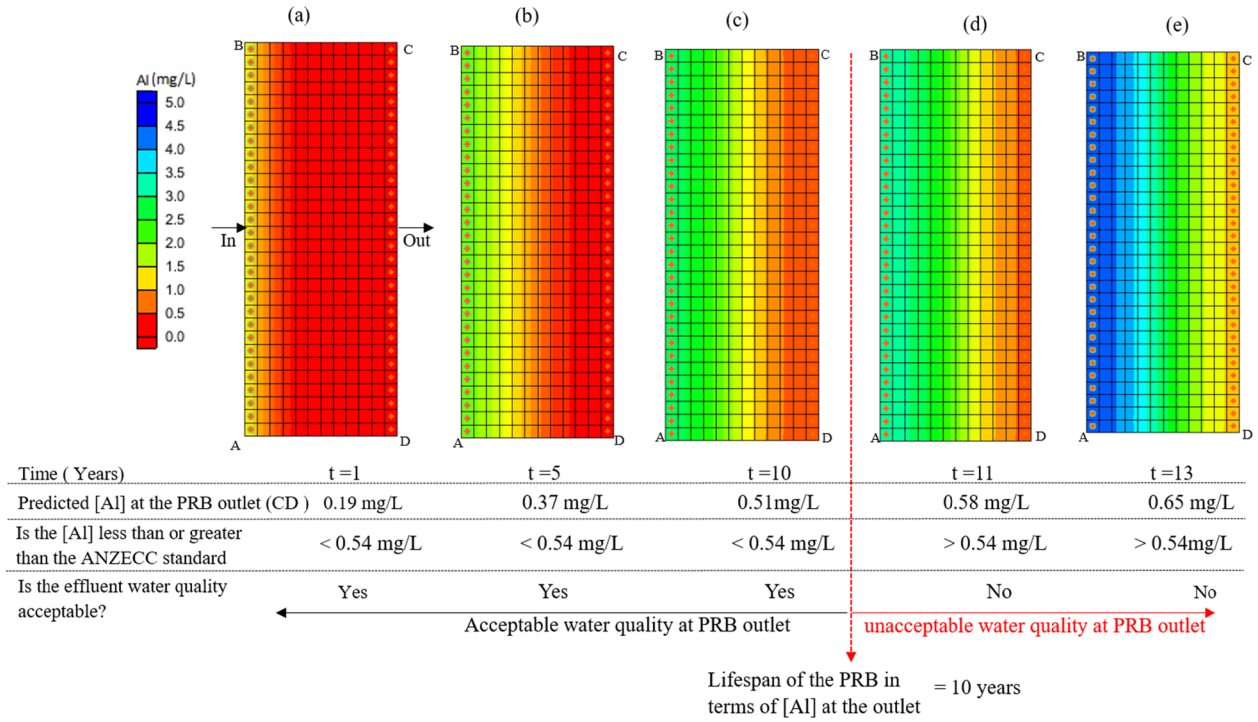

Fig. 7. Longevity prediction of PRB-1 (recycled concrete) based on Al^{3+} concentration (a) variation of [Al^{3+}] in ABCD layer at the end of 1st year (b) 5th year (c) 10th year (d) 11th year (e) 13th year.

16 years (Fig. 10d), whereas the pH at the outlet becomes acidic in the 17th year (Fig. 10e). Therefore, PRB-2 is expected to generate a near-neutral effluent over the first 16 years.

In conclusion, PRB-2 is expected to have an overall acid neutralising and toxic metal removal ability for about 16 years, after which the effluent water quality will degrade. However, the concentration of total Fe (Fig. 8) and Al^{3+} (Fig. 9) at the inlet is expected to increase considerably from the 5th year and thus reduce the pH (Fig. 10). Therefore, if the limestone aggregates at the inlet are replenished after about five years, the entrance zone should be reactivated, and the outlet may also improve in terms of removing contaminants, all of which would increase the lifespan of this PRB filled with limestone aggregates to more than 16 years.

For the same influent characteristics and dimensions, the longevity

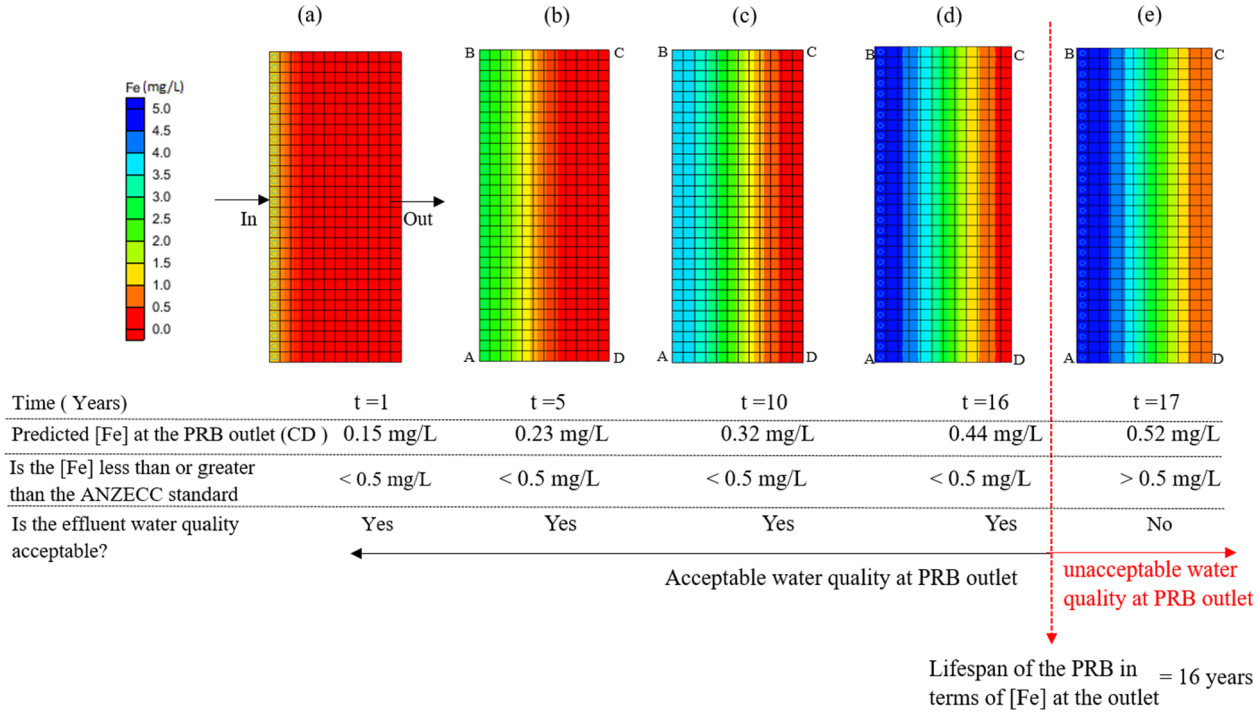

Fig. 8. Longevity prediction of PRB-2 (limestone) based on total Fe concentration (a) variation of [total Fe] in ABCD layer at the end of 1st year (b) 5th year (c) 10th year (d) 16th year (e) 17th year.

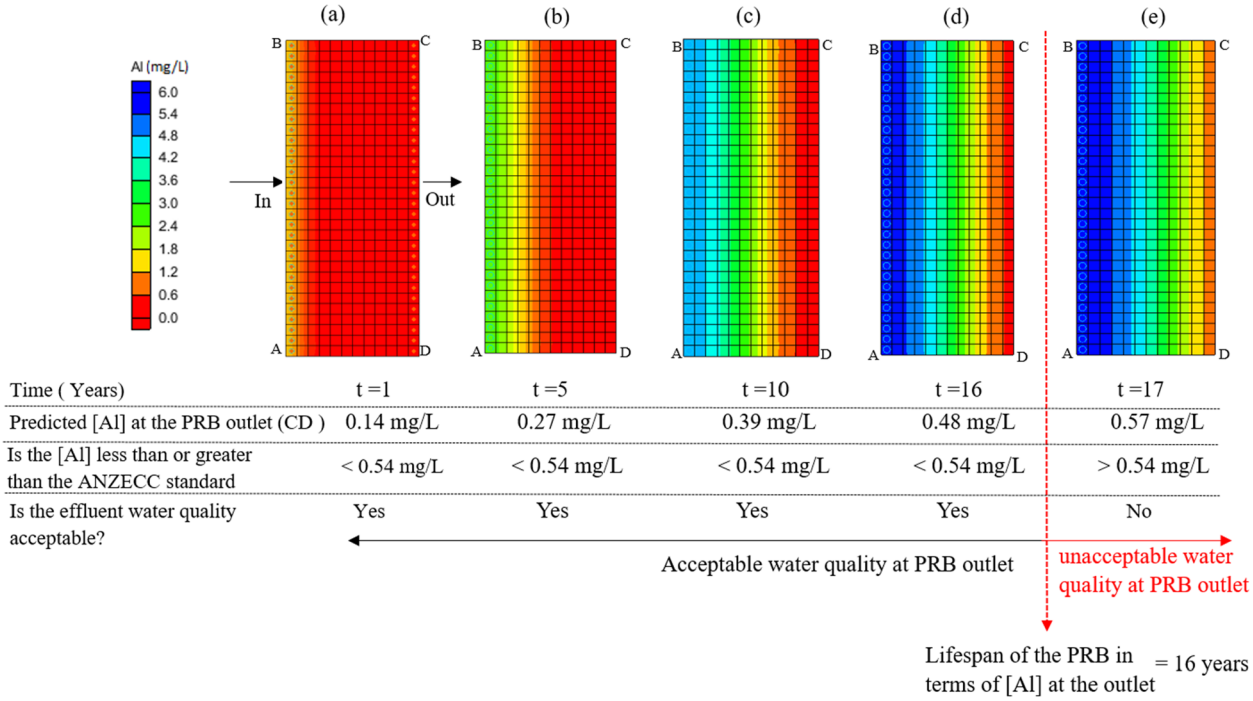

Fig. 9. Longevity prediction PRB-2 (limestone) based on Al^{3+} concentration (a) variation of [Al^{3+}] in ABCD layer at the end of 1st year (b) 5th year (c) 10th year (d) 16th year (e) 17th year.

predicted by the bio-geochemical model for a PRB filled with limestone aggregates should have a longer lifespan (about 16 years), than a PRB filled with recycled concrete aggregates (10 years). Note that recycled materials are subjected to the effects of ageing, and their chemical composition may vary from one batch to another, whereas the chemical properties of fresh limestone are usually more consistent such that the chemical treatment is expected to last longer than that based on aged concrete aggregates.

5. Comparison of geochemical model and bio-geochemical model

Indraratna et al. [6] applied their reactive transport model along the centreline of PRB-1 for the water quality parameters observed in the year 2012. Variations of porosity at each time step were introduced

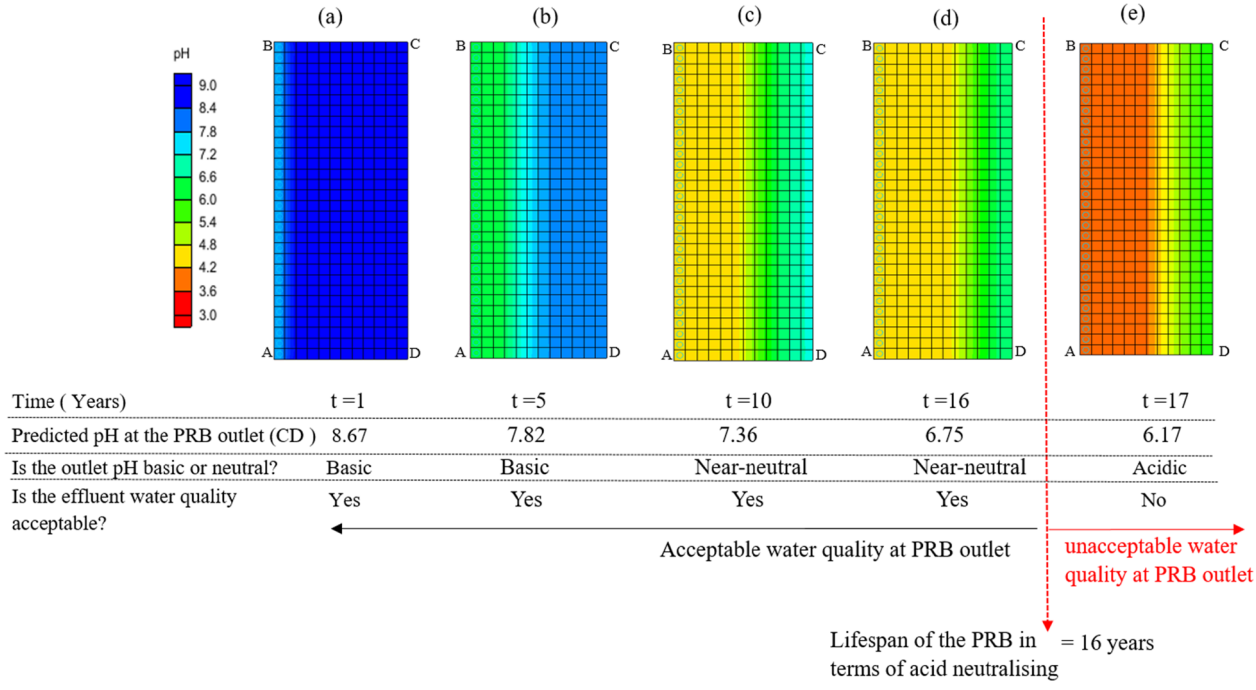

Fig. 10. Longevity prediction of PRB-2 (limestone) based on the acid neutralising properties (a)variation of the pH in ABCD layer at the end of 1st year (b) 5th year (c) 10th year (d) 16th year (e) 17th year.

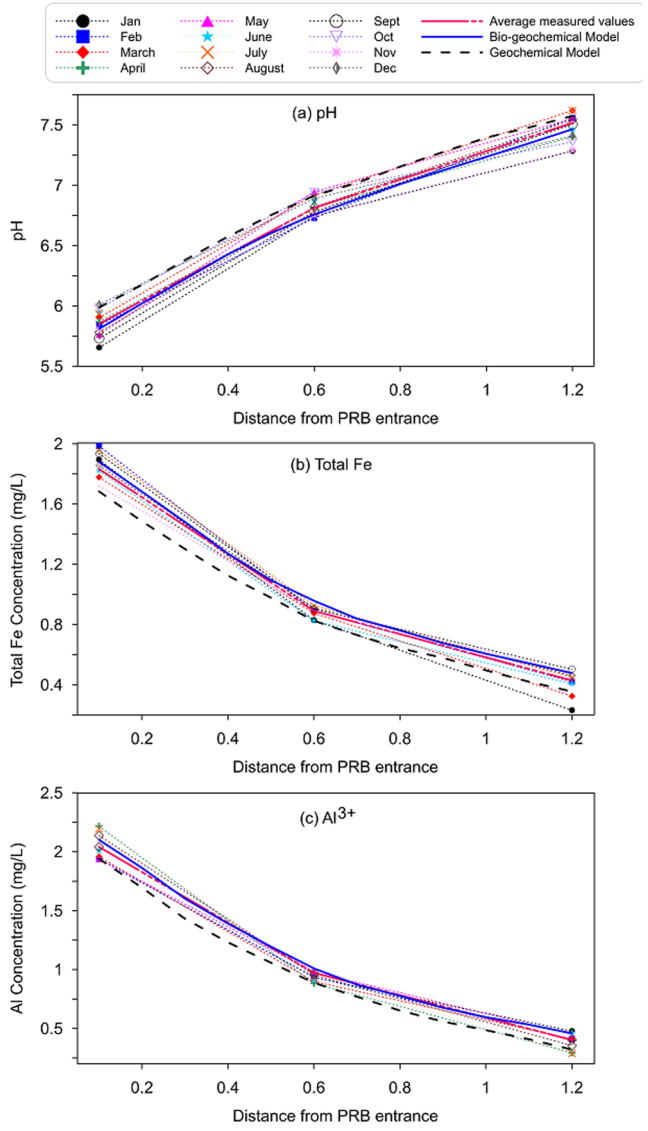

Fig. 11. Comparison between the geochemical model [6] and the bio-geochemical model with respect to the measured field data along the transect 3 of PRB-1 in 2012 (a) pH (b) Total Fe (c) Al^{3+}.

using the following to evaluate chemical clogging [6], which unlike Eq. (5), captured bio-geochemical clogging in the current model:

$$n_t = n_0 - \sum_{k=1}^{N_m} M_k R_k t \tag{14}$$

The bio-geochemical model was applied to the centreline of PRB-1 to determine the treatment pattern in 2012 and then compared with the predictions made by the previous geochemical model [6] for the same year. The differences between the two models are shown in Fig. 11a, b, and c, which indicate the removal of acidity, dissolved Al^{3+} and total Fe from groundwater. The pH and the concentrations of dissolved Al^{3+} and total Fe predicted by the current model conformed with the measured values, particularly at the entrance, whereas the previous model deviated from the measured values.

There is a noticeable gap between the predictions obtained by the two models, because, the equations for time-dependent hydraulic conductivity and porosity used in the geochemical model did not capture the catalysing effect of bacteria on mineral precipitation and accumulation of biomass inside the voids, resulting in less depletion of alkalinity and clogging compared to the results from the novel bio-geochemical model. Also, Indraratna et al. [7] directly used laboratory scale rate kinetics in the field predictions without scaling them up, which caused errors in the numerical procedure due to the scale effect. Furthermore, the growth of bacteria at the inlet is higher than that at the outlet because the load of nutrient supplement at the influent is higher [16]. Therefore, the effect of biological clogging on the overall reduction in porosity and hydraulic conductivity should be greater at the inlet. When the pH of the water increased, and the concentration of total Fe decreased non-homogeneously towards the outlet, the ability of bacteria to reduce the permeability of the granular assembly decreased towards the outlet. Therefore the difference between the predictions made from the geochemical and bio-geochemical models for the inlet of PRB-1 is larger than this difference in predictions at the outlet (Fig. 11).

Overall, the geochemical model predicted better water quality than actually existed, and, therefore, the predicted longevity was inaccurate. For example, the average concentration of total Fe measured at the PRB outlet in 2012 was 0.44 mg/L, and the bio-geochemical model predicted the concentration to be 0.48 mg/L, whereas the geochemical model predicted 0.41 mg/L (Fig. 11b). The average concentration of Al^{3+}measured at the outlet was 0.47 mg/L, whereas the bio-geochemical and geochemical model predicted 0.51 mg/L and 0.42 mg/L (Fig. 11c). On this basis, the predictions made from the newly developed bio-geochemical model were at least 9% greater than the actual field values and, hence, the lifespan of PRB-1 could be conservatively determined. The overall lifespan predicted for PRB-1 by the geochemical model was 19 years [6], but only 10 years by the bio-geochemical model (see Section 3.5). This difference stems from the reasons previously explained, but primarily from ignoring the microbial activity within the PRB.

6. Significance of the bio-geochemical model

Fig. 12 summarises how the bio-geochemical reactive transport model predicted the longevity of a proposed PRB, evaluated the performance of an existing PRB, and checked the accuracy of laboratory-scale kinetic rates. To the best of the authors' knowledge, this is the first time a numerical approach which combines all the biological and chemical reactions that occur inside a particular porous matrix has been used to determine the longevity of a PRB. On this basis, the bio-geochemical reactive transport model is useful for predicting the performance of a PRB in the design stage, and can also be used to determine the reaction rate coefficients and longevity of an existing PRB. If the predicted lifespan is not sufficient for a field application from an economic perspective, the initial dimensions can be changed, and the simulation repeated until the predictions for effluent concentrations meet the standards required for a particular area, while still having sufficient longevity.

7. Limitations of the approach used for longevity analysis

The maximum acidity (i.e. the lowest pH) and the maximum concentrations of the two major contaminant species (i.e. Al^{3+} and total Fe) recorded during the site monitoring were introduced as the model inputs along the PRB centreline to make the model conservative, albeit these parameters will decrease towards the outlet (Sections 3 and 4). Also, crossflows or flow divergence away from the centreline were assumed to be minimal. In view of this, the maximum recorded

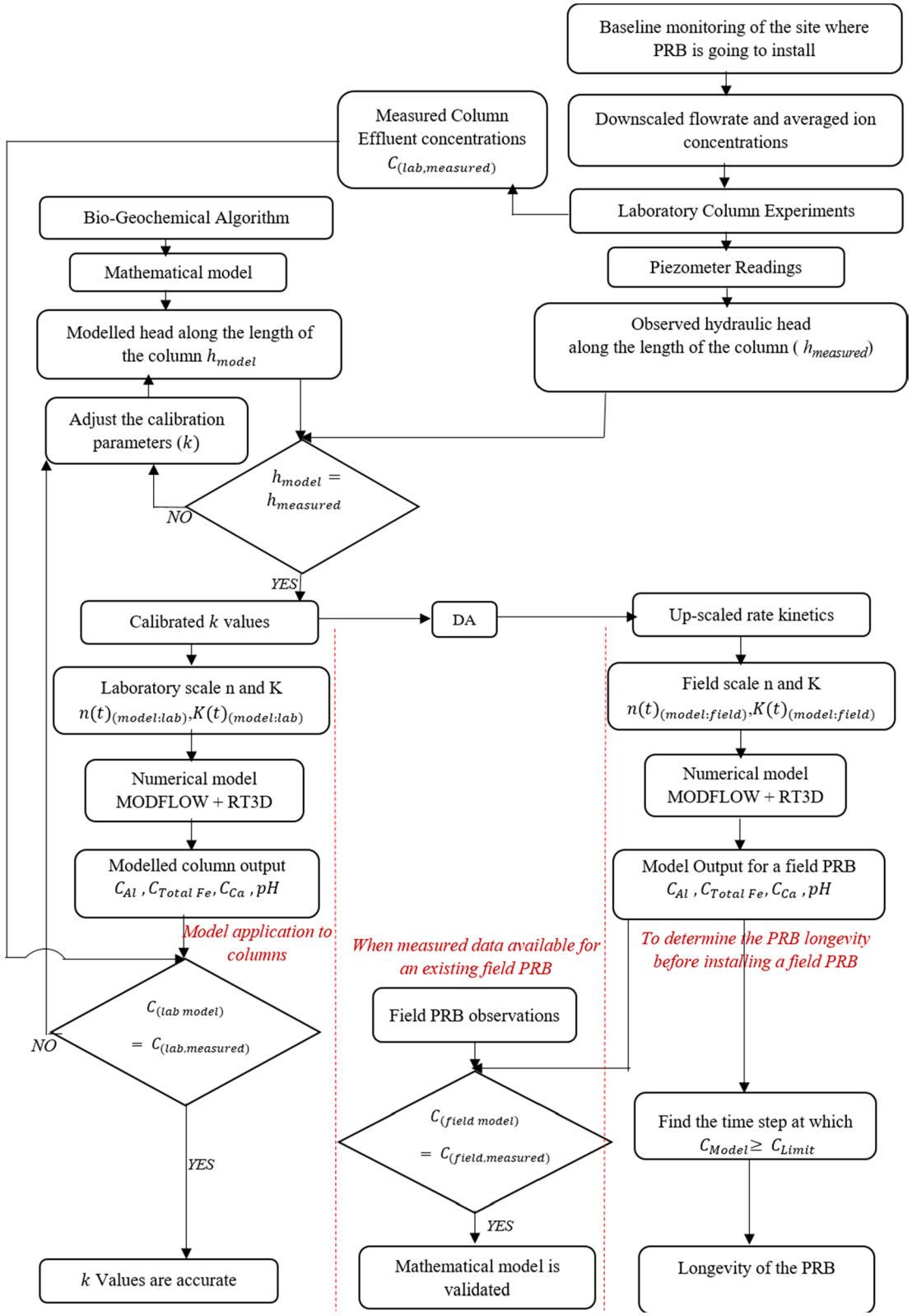

Fig. 12. Development of multi-component reactive transport model to determine the longevity of PRB.

magnitudes of the input parameters are assumed to remain the same, for any other transect taken parallel to the PRB centreline (see Fig. 1). Therefore, the same lifespan is determined by the model for all parallel transects. However, more sophisticated longevity calculations are possible for large scale industrial applications by introducing temporal variations of pH, concentrations of Al^{3+}, total Fe and reaction rate kinetics along the centreline, as well as localised variations of these input characteristics relevant to each transect of the PRB. Slightly different life spans would be determined for each transect according to the different input parameters, with the average being the final result. Although this approach complicates the model, resulting in more time-consuming convergence, the model still would be useful for providing a conservative simulation of the bio-geochemical clogging of a PRB.

8. Conclusions

The current study suggested an innovative numerical approach to predict the longevity of a PRB used for treating acidic groundwater. The proposed model was able to comprehensively examine and quantitatively analyse the occurrence of chemical and biological clogging in the PRB reactive medium. In this particular study, the dissolution potential of calcitic limestone and recycled concrete to release sufficient alkalinity and the corresponding precipitation potential of Fe and Al from the acidic groundwater could be effectively modelled under the influence of microbial growth. For instance, a previous geochemical model calculated nearly 18% lower concentrations of toxic metals (i.e. Fe and Al) than the measured values, hence overestimating the actual lifespan of the PRB. When the biological clogging is introduced, the current bio-geochemical model conservatively computed at least 9% higher metal concentrations than the field observations.

According to the model results for a PRB of dimensions 18 m × 1.2 m by 3 m to be installed in the Shoalhaven floodplain and filled with calcitic limestone aggregates, the PRB outlet was able to maintain acceptable standards of pH, concentrations of total Fe and Al^{3+} for over 15 years. Furthermore, the current model verified that the reactivity of inlet aggregates would diminish faster within one-third of the total lifespan caused by bio-geochemical clogging, compared to lesser fouling at the outlet.

The kinetic rates of chemical and biological reactions of a particular hydrogeological application should be determined based on considering whether the model is used for laboratory experiments or field conditions, because the lab-scale kinetic rates determined in this current study were almost three times greater than the field-scale kinetics.

9. Data Statement

Software used in the study and the methodology are described in the paper. Codes generated and used during the study are given in Appendices.

Field observations and data used in the study (presented in graphs) are available from the corresponding author by request.

CRediT authorship contribution statement

Subhani Medawela: Methodology, Software, Formal analysis, Investigation, Writing - original draft. **Buddhima Indraratna:** Supervision, Conceptualization, Resources, Writing - review & editing, Funding acquisition.

Declaration of Competing Interest

The authors declare that they have no known competing financial interests or personal relationships that could have appeared to influence the work reported in this paper.

Acknowledgement

The authors are grateful for funding received from the Australian Research Council (ARC) to support the research in this area. The guidance and support from Dr ana Heitor throughout the research is much appreciated. Authors are thankful to Professor Kerry Rowe for reviewing this research work. Authors are grateful for assistance from industry partners, with special thanks to Glenys Lugg from the Manildra Group and Paul Amidy from Glencore. The efforts of UOW technical staff and more than a dozen past PhD and Honours thesis students' research work in the field of acid sulphate soils are gratefully acknowledged.

Appendix A. Modification of bio-geochemical algorithm for recycled concrete

Indraratna et al. [16] developed a bio-geochemical algorithm for chemical and biological reactions occurred in a granular limestone assembly. Following the same approach, the geochemical algorithm developed by Indraratna et al. [7] for recycled concrete was modified to include the biological oxidation reactions that occur inside a PRB. Mineral dissolution and precipitation reactions are shown in Table A1. Reactions for the formation of Fe and Al oxides/hydroxides and the effect of bacteria on Fe oxidising in the granular waste concrete assembly are similar to what occurs inside limestone media despite the differences in reaction kinetic rates.

Following the procedure explained by Indraratna et al. [16], expressions were developed for individual reaction rates (r) of the reactions occur inside a recycled concrete granular assembly (Table A1). Then, the overall reaction rates (R_k) for each species (i.e. R_{Ca}, R_{Al}, $R_{Fe^{3+}}$ and $R_{Fe^{2+}}$) can be calculated using the following equations.

$$R_{Ca} = \frac{d[Ca^{2+}]}{dt} = -r_{1[Ca^{2+}]} - r_{2[Ca^{2+}Al^{3+}]} - r_{3[Ca^{2+}]} + r_{4[Ca^{2+}]} \quad (A.1)$$

$$R_{Al} = \frac{d[Al^{3+}]}{dt} = r_{1[Al^{3+}]} - r_{2[Ca^{2+}Al^{3+}]} \quad (A.2)$$

$$R_{Fe^{3+}} = \frac{d[Fe^{3+}]}{dt} = r_{1[Fe^{3+}]} + r_{2[Fe^{3+}]} + 2r_{3[Fe^{3+}]} + r_{[Fe^{2+}_{(aq)}]Chemical} + r_{[Fe^{2+}_{(aq)}]microbial} \quad (A.3)$$

$$R_{Fe^{2+}} = \frac{d[Fe^{2+}]}{dt} = 2r_{1[Fe^{2+}]} + 2r_{2[Fe^{2+}]} - r_{[Fe^{2+}_{(aq)}]Chemical} - r_{[Fe^{3+}_{(aq)}]microbial} \quad (A.4)$$

The kinetic rate coefficients (k) of reactions shown in Table A1 for a PRB filled with recycled concrete were determined by calibrating the mathematical model proposed by Indraratna et al. [16], and the values are given Table 1.

Table A1
Bio-geochemical reactions occurred in recycled concrete.
Source Indraratna et al. [7]).

Reaction type	Reaction	Overall reaction Rate
Dissolution of Ca bearing minerals from recycled concrete	$Ca(OH)_2 + 2H^+ \leftrightarrow Ca^{2+} + 2H_2O$	$\frac{d[m_{Ca(OH)_2}]}{dt} = \frac{1}{2}\frac{d[H^+]}{dt} = -\frac{d[Ca^{2+}]}{dt} = r_{1[Ca^{2+}]} = k_{[Ca^{2+}]}\left[\frac{a_{Ca^{2+}}a^2_{OH^-}}{k_{eq,Ca^{2+},OH^-}} - 1\right]$
	$CaAl_2Si_2O_8 + 8H^+ \leftrightarrow Ca^{2+} + 2Al^{3+} + 2H_4SiO_4$	$\frac{d[m_{CaAl_2Si_2O_8}]}{dt} = \frac{1}{8}\frac{d[H^+]}{dt} = -\frac{d[Ca^{2+}]}{dt} = -\frac{1}{2}\frac{d[Al^{3+}]}{dt} = r_{2[Ca^{2+}Al^{3+}]} = k_{[Ca^{2+}Al^{3+}]}\left[\frac{a_{Ca^{2+}}a^2_{Al^{3+}}}{k_{eq,Ca^{2+}Al^{3+}}} - 1\right]$
	$CaCO_3 + 2H^+ \leftrightarrow Ca^{2+} + H_2$	$\frac{d[m_{CaCO_3}]}{dt} = \frac{1}{2}\frac{d[H^+]}{dt} = -\frac{d[Ca^{2+}]}{dt} = -\frac{d[H_2CO_3]}{dt}r_{3[Ca^{2+}]} = k_{[Ca^{2+}]}\left[\frac{a_{Ca^{2+}}a_{CO_3^{2-}}}{k_{eq[Ca^{2+}]}} - 1\right]$
Chemical/ aerobic ferrous oxidation	$Fe^{2+}_{(aq)} + \frac{1}{4}O_{2(aq)} + H^+_{(aq)} \rightarrow Fe^{3+}_{(aq)} + \frac{1}{2}H_2O$	$-\frac{d[Fe^{2+}_{(aq)}]}{dt} = -\frac{1}{4}\frac{d[O_{2(aq)}]}{dt} = -\frac{d[H^+]}{dt} = \frac{d[Fe^{3+}]}{dt} = r_{[Fe^{2+}_{(aq)}]Chemical} = k_{che}\left[\frac{a_{Fe^{3+}}}{k_{eqa_{Fe^{3+}}}} - 1\right]$
Microbial ferrous oxidation	$Fe^{2+}_{(aq)} + \frac{1}{4}O_{2(aq)} + H^+_{(aq)} \xrightarrow{Bacteria} Fe^{3+}_{(aq)} + \frac{1}{2}H_2O$	$-\frac{d[Fe^{2+}_{(aq)}]}{dt} = -\frac{1}{4}\frac{d[O_{2(aq)}]}{dt} = -\frac{d[H^+]}{dt} = \frac{d[Fe^{3+}]}{dt} = r_{[Fe^{2+}_{(aq)}]microbial} = k_{bio}\left(\frac{[Fe^{2+}_{(aq)}]}{K_{\left(Fe^{2+}_{(aq)}\right)} + [Fe^{2+}_{(aq)}]}\right)\left(\frac{[O_{2(aq)}]}{KO_2 + [O_{2(aq)}]}\right)\left(\frac{[H^+]}{K_{H^+} + [H^+]}\right)$
Mineral precipitates in recycled concrete granular assembly	$Fe^{3+} + 3H_2O \rightarrow Fe(OH)_{3(s)} + 3H^+_{(aq)}$	$\frac{d[Fe^{3+}]}{dt} = -\frac{d[m_{Fe(OH)_3}]}{dt} = -\frac{1}{3}\frac{d[H^+]}{dt} = r_{1[Fe^{3+}]} = k_{[Fe^{3+}]}\left[\frac{a_{Fe^{3+}}a^3_{OH^-}}{k_{eq,Fe^{3+},OH^-}} - 1\right]$
	$Fe^{3+} + 2H_2O \rightarrow FeO(OH) + 3H^+_{(aq)}$	$\frac{d[Fe^{3+}]}{dt} = -\frac{d[m_{FeOOH}]}{dt} = -\frac{1}{3}\frac{d[H^+]}{dt} = r_{2[Fe^{3+}]} = k_{[Fe^{3+}]}\left[\frac{a_{Fe^{3+}}a_{OOH^{3-}}}{k_{eq,Fe^{3+},OOH^{3-}}} - 1\right]$
	$2Fe^{3+} + 3H_2O \rightarrow Fe_2O_3 + 6H^+_{(aq)}$	$\frac{1}{2}\frac{d[Fe^{3+}]}{dt} = -\frac{d[m_{Fe_2O_3}]}{dt} = -\frac{1}{6}\frac{d[H^+]}{dt} = r_{3[Fe^{3+}]} = k_{[Fe^{3+}]}\left[\frac{a^2_{Fe^{3+}}a^3_{O^{2-}}}{k_{eq,Fe^{3+},O^{2-}}} - 1\right]$
	$Fe^{2+} + 2(OH)^- \leftrightarrow Fe(OH)_2$	$\frac{1}{2}\frac{d[Fe^{2+}]}{dt} = \frac{1}{2}\frac{d[OH^-]}{dt} = -\frac{d[m_{Fe(OH_2)}]}{dt} = r_{1[Fe^{2+}]} = k_{[Fe^{2+}]}\left[\frac{a_{Fe^{2+}}a^2_{OH^-}}{k_{eq,Fe^{2+},OH^-}} - 1\right]$
	$Fe^{2+} + CO_3^{2-} \leftrightarrow Fe(CO)_{3(s)}$	$\frac{d[Fe^{2+}]}{dt} = \frac{d[CO_3^{2-}]}{dt} = -\frac{d[m_{FeCO_3}]}{dt} = r_{2[Fe^{2+}]} = k_{[Fe^{2+}]}\left[\frac{a_{Fe^{2+}}a_{CO_3^{2-}}}{k_{eq,Fe^{2+},CO_3^{2-}}} - 1\right]$
	$Al^{3+} + 3H_2O \rightarrow Al(OH)_{3(s)} + 3H^+_{(aq)}$	$\frac{d[Al^{3+}]}{dt} = -\frac{d[m_{Al(OH)_3}]}{dt} = -\frac{1}{3}\frac{d[H^+]}{dt} = r_{1[Al^{3+}]} = k_{[Al^{3+}]}\left[\frac{a_{Al^{3+}}a^3_{OH^-}}{k_{eq,Al^{3+},OH^-}} - 1\right]$
	$Ca(OH)_2 + CO_2 \leftrightarrow CaCO_3 + H_2O$	$\frac{d[Ca^{2+}]}{dt} = \frac{d[CO_3^{2-}]}{dt} = -\frac{d[m_{CaCO_3}]}{dt} = r_{4[Ca^{2+}]} = k_{[Ca^{2+}]}\left[\frac{a_{Ca^{2+}}a_{CO_3^{2-}}}{k_{eq[Ca^{2+}]}} - 1\right]$

Appendix B. FORTRAN Subroutine for user-defined reaction module in RT3D

```
      SUBROUTINE rxns(ncomp,nvrxndata,j,i,k,y,dydt,
     &         poros,rhob,reta,rc,nlay,nrow,ncol,vrc)


c ***** Block 1: Comments block *******
c234567890123456789012345678901234567890123456789012345678901234567890123456789012
c ncomp - Total number of components
c nvrxndata - Total number of variable reaction parameters to be input via RCT file
c J, I, K - node location (used if reaction parameters are spatially variable)
c y - Concentration value of all component at the node [array variable y(ncomp)]
c dydt - Computed RHS of your differential equation [array variable dydt(ncomp)]
c poros - porosity of the node
c reta -  Retardation factor [array variable reta(mcomp)]
c rhob -  bulk density of the node
c rc - Stores spatially constant reaction parameters (up to 100 values)
c nlay, nrow, ncol - Grid size (used only for dimensioning purposes)
c vrc - Array variable that stores spatially variable reaction parameters
c ***** End of Block 1 *******

c *** Block 2: Please do not modify this standard interface block ***
    !MS$ATTRIBUTES DLLEXPORT :: rxns
      IMPLICIT NONE
      INTEGER ncol,nrow,nlay
      INTEGER ncomp,nvrxndata,j,i,k
      INTEGER First_time
      DATA First_time/1/
      DOUBLE PRECISION y,dydt,poros,rhob,reta
      DOUBLE PRECISION rc,vrc
      DIMENSION y(ncomp),dydt(ncomp),rc(50)
      DIMENSION vrc(ncol,nrow,nlay,nvrxndata),reta(50)
C ****** End of block 2 *******

C *** Block 3: variables ***
      DOUBLE PRECISION TBF,kbio,X ! bacteria
      DOUBLE PRECISION Ca,kc,Sc ! [Ca]
      DOUBLE PRECISION Al,ka,Sa ! [Al]
      DOUBLE PRECISION Fe,kf,kff,kfff,Sf,Sff,Sfff ![Fe3+]
      DOUBLE PRECISION FERROUS,kp,kpp,Sp,Spp ! [Fe2+]
      DOUBLE PRECISION p,b,kpc,kpb,Spc,Spb ! chemical and biological
      DOUBLE PRECISION FeHydroxide, Goethite, Hematite,FeOH,Siderite
      DOUBLE PRECISION HI,HII ! pH

C ***** End of Block 3  ******

C *** Block 4: reaction parameters ***
      IF (First_time .EQ. 1) THEN

        kc = rc(1) !CaCO3
        ka = rc(2) !AlOH3
        kf = rc(3) !FeOH3
        kff = rc(4) !FeOOH
        kfff = rc(5) !Fe2O3
        kp = rc(6) !Fe(OH)2
        kpp = rc(7) !FeCO3
        kpc = rc(8) !Chem
        kpb = rc(9) !bio
        X   = rc(10) !TBF


         First_time = 0 !reset First_time to skip this block later
      END IF
```

```
C ***** End of Block 4  ******

C  *** Block 5: other variable names ***

      Ca = y(1)
      Al = y(2)
      FeHydroxide = y(3)
      Goethite= y(4)
      Hematite= y(5)
      FeOH = y(6)
      Siderite = y(7)
      p = y(8)
      b = y(9)
      Fe = y(10)
      FERROUS = y(11)
      TBF = y(12)
      HI = y(13)
      HII = y(14)
      Sc = rc(11)
      Sa = rc(12)
      Sf = rc(13)
      Sff = rc(14)
      Sfff = rc(15)
      Sp = rc(16)
      Spp = rc(17)
      Spc = rc(18)
      Spb = rc(19)
      kbio = rc(20)

    C ***** End of Block 5  ******

c  *** Block 6: Differential Equations ***

      dydt(1) = 4*kc*Sc
      dydt(2) = ka*Sa
      dydt(3) = kf*Sf
      dydt(4) = kff*Sff
      dydt(5) = kfff*Sfff
      dydt(6) = kp*Sp
      dydt(7) = kpp*Spp
      dydt(8) = kpc*Spc
      dydt(9) = kpb*Spb
      dydt(10) = dydt(3)+dydt(4)+dydt(5)+dydt(8)+dydt(9)
      dydt(11) = 2*dydt(6)+2*dydt(7)-dydt(8)-dydt(9)
      dydt(12) = kbio*TBF*(X-TBF)*0.00000005
      dydt(13) = dydt(1)*0.25-dydt(8)-dydt(9)-3*dydt(3)-3*dydt(4)
      dydt(14) = -6*dydt(5)-3*dydt(2)

C ***** End of Block 6  ******
      RETURN
      END
```

References

[1] Fanning DS, Rabenhorst MC, Fitzpatrick RW. Historical developments in the understanding of acid sulfate soils. Geoderma 2017;308:191–206.

[2] Gavaskar AR. Design and construction techniques for permeable reactive barriers. J Hazard Mater 1999;68:41–71.

[3] Indraratna B, Regmi G, Nghiem LD, Golab A. Performance of a PRB for the remediation of acidic groundwater in acid sulfate soil terrain. J Geotech Geoenviron Eng, ASCE 2010;136:897–906.

[4] Golab AN, Indraratna B, Peterson MA, Hay S. Design of a permeable reactive barrier to remediate acidic groundwater. ASEG Extended Abstr 2006:1–3.

[5] Medawela S, Indraratna B, Pathirage U, Heitor A. Controlling soil and water acidity in acid sulfate soil terrains using permeable reactive barriers. Geotechnics for transportation infrastructure. Singapore: Springer; 2019. p. 413–26.

[6] Gavaskar A, Yoon W, Sminchak J, Sass B, Gupta N, Hicks J, et al. Long Term Performance Assessment of a Permeable Reactive Barrier at Former Naval AITR Station Moffett Field. DTIC Document; 2005.

[7] Indraratna B, Pathirage PU, Rowe RK, Banasiak L. Coupled hydro-geochemical modelling of a permeable reactive barrier for treating acidic groundwater. Comput Geotech 2014;55:429–39.

[8] Li L, Benson CH. Impact of fouling on the long-term hydraulic behaviour of permeable reactive barriers. IAHS Publ 2005;298:23.

[9] Indraratna B, Medawela S, Athuraliya S, Heitor A, Baral P. Chemical clogging of granular media under acidic groundwater. Environmental Geotechnics, Special Issue: Testing and Modelling of Complex Rockfill Material (Ahead of print); 2019. DOI: 10.1680/JENGE.18.00143.

[10] Cravotta III, CA, Watzlaf GR. Design and performance of limestone drains to increase pH and remove metals from acidic mine drainage. Handbook of Groundwater Remediation Using Permeable Reactive Barriers; 2002, 19–66.

[11] Nordstrom DK. Aqueous pyrite oxidation and the consequent formation of secondary iron minerals. Acid Sulfate Weathering 1982:37–56.
[12] Arkesteyn GJ. Pyrite oxidation in acid sulphate soils: The role of miroorganisms. Plant Soil 1980;54:119–34.
[13] Rawlings DE. Heavy metal mining using microbes 1. Ann Rev Microbiol 2002;56:65–91.
[14] Harbaugh AW. MODFLOW-2005, the US Geological Survey modular ground-water model: the ground- water flow process, US Department of the Interior, US Geological Survey Reston, VA, USA; 2005.
[15] Clemen, TP. A modular computer code for simulating reactive multi-species transport in 3-dimensional groundwater systems. Pacific Northwest National Laboratory, vol. 11720; 1997.
[16] Indraratna B, Medawela S, Rowe RK, Thamwattana N, Heitor A. Bio-Geochemical clogging of Permeable Reactive Barriers in Acid Sulfate Soil Floodplain. J Geotech Geoenviron Eng, ASCE 2020;146(5)https://ascelibrary.org/doi/10.1061/%28ASCE%29GT.1943-5606.0002231.
[17] Li L, Benson CH, Lawson EM. Modeling porosity reductions caused by mineral fouling in continuous-wall permeable reactive barriers. J Contam Hydrol 2006;83:89–121.
[18] Mayer K, Benner S, Blowes D. Process-based reactive transport modeling of a permeable reactive barrier for the treatment of mine drainage. J Contam Hydrol 2006;85(3):195–211.
[19] Parkhurst DL, Appelo C. User's guide to PHREEQC (Version 2): A computer program for speciation, batch-reaction, one-dimensional transport, and inverse geochemical calculations. Water-Resour Investigations Report 1999;99:312.
[20] Li L, Peters CA, Celia MA. Upscaling geochemical reaction rates using pore-scale network modeling. Adv Water Resour 2006;29:1351–70.
[21] Hochstetler DL, Kitanidis PK. The behavior of effective rate constants for bimolecular reactions in an asymptotic transport regime. J Contam Hydrol 2013;144(1):88–98.
[22] Lichtner PC, Tartakovsky D. Stochastic analysis of effective rate constant for heterogeneous reactions. Stoch Env Res Risk Assess 2003;17(6):419–29.
[23] Tartakovsky DM, Dentz M, Lichtner PC. Probability density functions for advective-reactive transport with uncertain reaction rates. Water Resour Res 2009; 45.
[24] Monod J. The growth of bacterial cultures. Ann Rev Microbiol 1949;3(1):371–94.
[25] Indraratna B, Pathirage PU, Banasiak LJ. Remediation of acidic groundwater by way of permeable reactive barrier. Environ Geotech 2014;4(4):284–98.
[26] Regmi G, Indraratna B, Nghiem LD. Long-term performance of a permeable reactive barrier in acid sulphate soil terrain. Water Air Soil Pollut Focus 2009;9:409–19.
[27] Pathirage U, Indraratna B. Assessment of optimum width and longevity of a permeable reactive barrier installed in an acid sulfate soil terrain. Can Geotech J 2014;52:999–1004.
[28] ANZECC A. Australian and New Zealand guidelines for fresh and marine water quality. Australian and New Zealand Environment and Conservation Council and Agriculture and Resource Management Council of Australia and New Zealand, Canberra; 2000, 1–103.